J. Membrane Biol. 168, 63–75 (1999)

The Journal of
Membrane
Biology

An Energy-Barrier Model for the Permeation of Monovalent and Divalent Cations Through the Maxi Cation Channel in the Plasma Membrane of Rye Roots

P.J. White[1], **M.S. Ridout**[2]

[1]Department of Cell Physiology, Horticulture Research International, Wellesbourne, Warwick CV35 9EF, UK
[2]Department of Biometrics, Horticulture Research International, East Malling, West Malling, Kent ME19 6BJ, UK

Received: 29 April 1998/Revised: 20 November 1998

Abstract. The depolarization-activated, high-conductance "maxi" cation channel in the plasma membrane of rye (*Secale cereale* L.) roots is permeable to a wide variety of monovalent and divalent cations. The permeation of K^+, Na^+, Ca^{2+} and Ba^{2+} through the pore could be simulated using a model composed of three energy barriers and two ion binding sites (a 3B2S model), which assumed single-file permeation and the possibility of double cation occupancy. The model had an asymmetrical free energy profile. Differences in permeation between cations were attributed primarily to differences in their free energy profiles in the regions of the pore adjacent to the extracellular solution. In particular, the height of the central free energy peak differed between cations, and cations differed in their affinities for ion binding sites. Significant ion repulsion occurred within the pore, and the mouths of the pore had considerable surface charge. The model adequately described the diverse current *vs.* voltage (*I/V*) relationships obtained over a wide variety of experimental conditions. It described the phenomena of non-Michaelian unitary conductance *vs.* activity relationships for K^+, Na^+ and Ca^{2+}, differences in selectivity sequences obtained from measurements of conductance and permeability ratios, changes in relative cation permeabilities with solution composition, and the complex effects of Ba^{2+} and Ca^{2+} on K^+ currents through the channel. The model enabled the prediction of unitary currents and ion fluxes through the maxi cation channel under physiological conditions. It could be used, in combination with data on the kinetics of the channel, as input to electrocoupling models allowing the relationships between membrane voltage, Ca^{2+} influx and Ca^{2+} signaling to be studied theoretically.

Correspondence to: P.J. White

Key words: Calcium (Ca^{2+}) — Maxi cation channel — Permeation — Planar Lipid Bilayer — Potassium (K^+) — Rye (*Secale cereale* L.)

Introduction

When plasma membrane vesicles from rye (*Secale cereale* L.) roots are incorporated into planar lipid bilayers (PLB) a high-conductance, voltage-dependent "maxi" cation channel is frequently observed (White, 1997). This channel is permeable to a wide variety of monovalent and divalent cations and is activated by membrane depolarization (White, 1993). Its physiological role may be to sense, and initiate cellular responses to, diverse environmental, developmental or pathological stimuli by mediating Ca^{2+} influx upon plasma membrane depolarization (White, 1997, 1998*a*). An understanding of cation permeation, and an ability to predict the current and ionic fluxes through the maxi cation channel under physiological conditions, would allow a theoretical examination of the involvement of the maxi cation channel in depolarization-mediated Ca^{2+} signaling.

In this paper free energy profiles describing the permeation of K^+, Na^+, Ca^{2+} and Ba^{2+} through the pore of the maxi cation channel are presented. These are based on a three-energy-barrier, two-ion-binding-site (3B2S) model (Alvarez, Villarroel & Eisenman, 1992). This model is based on a pore structure, such as the *Shaker*-type selectivity filter, which can contain two cations simultaneously and, thereby, exploits electrostatic repulsion to promote cation conduction (Doyle et al., 1998). The phenomena of nonsaturating conductance *vs.* activity relationships (White, 1993), differences in selectivity sequences obtained from measurements of conductance and permeability ratios (White, 1993), changes in relative cation permeabilities with absolute concentration

(White, 1997) and electrical distances for verapamil and quinine blockade which are greater than unity (White & Ridout, 1998; White, 1998*b*) all suggest that the pore of the maxi cation channel can contain more than one ion, and that ions occupying the pore simultaneously interact with each other.

The proposed 3B2S permeation model enables the prediction of unitary currents and ion fluxes through the maxi cation channel under physiological conditions. This will be useful in dissecting cell signaling processes and electrocoupling in the plasma membrane.

Materials and Methods

Plant Material and Plasma Membrane Isolation

Rye (*Secale cereale* L.) was grown hydroponically in a complete nutrient medium containing 400 μM K^+ (White, 1993, 1996). Plants were harvested 14 d after sowing and plasma-membrane vesicles were obtained by aqueous-polymer two-phase partitioning of a root microsomal-membrane fraction (White, 1993, 1996).

Recording Ion Channel Activities

Plasma-membrane vesicles were incorporated into PLB composed of 30 mM synthetic 1-palmitoyl-2-oleoyl phosphatidylethanolamine (PE) dispersed in n-decane in the presence of a (*cis:trans*) 300:100 mM KCl gradient following their addition to the *cis* chamber (White, 1993). When channel activity was detected, unfused vesicles were removed by perfusing the *cis* chamber with 100 mM KCl. Further changes in the ionic composition of solutions were effected either by perfusing with appropriate solutions or by adding aliquots of concentrated stock solutions (100 mM or 1 M for divalent cations; 3 M for KCl). Aqueous solutions were buffered with 5 mM N-tris-[hydroxymethyl]-methyl-2-aminoethane sulfonic acid (TES), titrated to pH 7.5 using *N*-methyl-D-glucamine. Experiments were performed at room temperature (approximately 20°C). Current was monitored under voltage-clamp conditions using a low noise operational amplifier with frequency compensation, connected to the bilayer chambers by calomel electrodes and 3 M KCl salt bridges. Data were stored on digital audiotape (DTC1000ES; 44.1 kHz per channel; Sony Corporation, Japan) and simulutaneously displayed on a digital storage oscilloscope (Gould 1602; Gould Electronics, Hainault, Essex, UK).

Membrane potentials were recorded *trans* with respect to *cis*. Since the cytoplasmic side of the plasma membrane faces the vesicle lumen and vesicles fuse with PLB such that the inside becomes exposed to the *trans* chamber, plasma-membrane ion channels become oriented with their cytoplasmic face exposed to the *trans* chamber (White, 1997). Thus, the sign of the membrane potential is in accordance with that conventionally used in electrophysiological experiments of plant cells in vivo. Movement of K^+ from the *cis* (extracellular) to the *trans* (cytoplasmic) chamber is indicated by a negative current.

The amplitude of single channel currents was determined directly from channel recordings filtered at 100 Hz using an 8-pole low pass Bessel filter (902LPF, Frequency Devices, Haverhill, MA). Although the maxi cation channel in the plasma membrane of rye roots has several discrete subconductance states (the most frequently observed approximating 12 and 93% of the maximal current; White 1993), *I/V* relationships shown here relate to the maximal unitary current recorded.

Modeling

Estimates of energy profiles for permeant cations and structural characteristics of the channel were obtained using a version of the FORTRAN computer program AJUSTE (Alvarez et al., 1992) modified for the presence of both monovalent and divalent cations. Similar modifications to AJUSTE to those described here were made by French et al. (1994) for their study of the permeation and blockade of Na^+ channels by Ca^{2+}. The model chosen (a 3B2S model) had energy profiles consisting of three energy barriers and two ion-binding sites (energy wells), and allowed for single-file permeation, double cation occupancy, ion-ion repulsion and surface potential effects. The energies of the unoccupied channel at zero voltage (expressed as multiples of the thermal energy, RT) were defined by three peaks G1, G2 and G3, and two wells, U1 and U2, with the postscript referring to their position relative to the *cis* (extracellular) compartment. The distances D1 to D5 refer to the position of successive peaks and wells in the electrical field relative to the *cis* compartment.

The effects of ion-ion interactions (electrostatic and/or allosteric) were simulated by the addition of an energy factor to the peaks and wells adjacent to an occupied well. The energy shift was calculated as $A(z_1z_2)/d$, where A is the ionic-repulsion energy parameter, z_1 and z_2 are the valencies of the interacting ions and d is the electrical distance from the occupied well, to mimic a coulombic interaction.

Two parameters (R_{scis} and R_{strans}) were included in the model to describe surface charge effects. These parameters correspond to the radii of circles (expressed in angstrom, Å units) containing one electron charge in the *cis* and *trans* vestibules of the pore respectively, from which the fixed surface charge densities at the vestibule of the pore can be calculated ($\sigma = e/\pi R_s^2$). Since the PE bilayer is essentially uncharged under the experimental conditions, surface potentials are assumed to arise from charged amino-acid side chains and/or nonprotein domains forming part of the molecular structure of the channel. The relationship between surface charge density (σ) and the electrostatic surface potential (ϕ_0), which represents a charged planar surface, is given by the equation (based on eq. 11 of Latorre, Labarca & Naranjo, 1992):

$$\sigma = \pm \frac{1}{272}\left[\sum_i C_i\,[\exp(-z_i F\phi_0/RT) - 1]\right]^{0.5}$$

where C_i is the concentration of the i^{th} ionic species, z_i is its valence and F, R and T have their usual meanings. This equation was used to calculate the surface potential, given the surface charge density. Because there is, in general, no explicit solution, the equation was solved numerically using the Newton-Raphson method.

The effect of applied voltage was modeled by addition of the zero-voltage energy to an electrical work term proportional to the valence of the ion and electrical distance. It was assumed that the electrical field, which is the algebraic sum of the electrical fields induced by the applied voltage and the asymmetry of the surface potential, dropped linearly through the energy profile and it was added point by point to compute the free energy of each peak and well. Rate constants for transitions between permissible states were formulated by the standard Eyring rate theory expression equal to the product of a pre-exponential term, kT/h (where k/h is Boltzmann's constant divided by Planck's constant), and an exponential function of the energy difference, $\exp(\Delta G/(RT))$. A similar expression was used for bimolecular rate constants describing the entry of ions from the internal or external solutions, except that the pre-exponential factor was also multiplied by

Table 1. Unitary conductances, determined between ±60 mV in the presence of symmetrical 100 mM cation chloride, of the maxi cation channel from the plasma membrane of rye roots studied in planar PE bilayers

Cation	Unitary conductance (pS)	
	Cambridge	HRI
K^+	436 ± 7.9 (43)	483 ± 4.9 (91)
Na^+	277 ± 9.3 (6)	298 ± 6.6 (3)
Ca^{2+}	151 ± 9.7 (3)	171 ± 9.7 (3)
Ba^{2+}	216 ± 7.9 (8)	195 (1)

Experiments were performed at the University of Cambridge and at HRI. Results are expressed as mean ± SE from the number of determinations in parentheses.

the molar activity of the ion in solution divided by the molar concentration of water (55.5 M). Thus, the reference energy state of our model corresponds to 55.5 M solution. To compare our energy values to models that use a 1 M reference state, 4.02 *RT* units must be added to our values.

Ionic activities were used for all calculations describing permeation. Geometric mean activity coefficients were taken from Robinson & Stokes (1959) and independent activity coefficients were calculated according to Margolis (1966). The concentrations of ions in the buffer solution were included in all calculations since they affect both ionic activities and surface potential through ionic strength effects.

Fitting Strategy

Parameters were estimated by unweighted least squares. Fitting began with a symmetrical model, with electrical distances of 0.00, 0.25, 0.50, 0.75 and 1.00 for D1 through D5, respectively. Starting parameters for well-depths were based on cation concentrations giving half-maximal conductance and for barrier heights on maximal cation conductances. At the outset, surface charge was minimized, but was systematically raised to reduce the RSS. Initially, models with fewer parameters were fitted to subsets of the data obtained in the presence of single cation species. These were then combined sequentially. Three contrasting sets of parameter estimates were pursued and the one with the lowest RSS is presented here. In total over 100 regressions were run in the course of developing the final model.

Standardization of Experimental Data

The data presented here were collected either at the Department of Botany, University of Cambridge, or at Horticulture Research International (HRI) over a period of seven years. Although the *I/V* relationships were qualitatively similar at both institutes, and similar ratios for unitary conductances in the presence of K^+, Na^+, Ca^{2+} and Ba^{2+} were obtained at Cambridge and at HRI, estimates of ionic currents were consistently lower at Cambridge than at HRI (see Table 1; *see also* White & Ridout, 1995). To facilitate modeling, ionic currents from individual experiments were scaled so that the unitary conductance determined between +60 and −60 mV in the presence of symmetrical 100 mM KCl was 482.5 pS. In addition to the data presented in the figures and figure legends, data were obtained in solutions containing (*cis:trans*) 300:100 mM KCl and 150:50, 50:50 and 263:100 mM $BaCl_2$ for the purposes of modeling. Original single-channel recordings of the maxi cation channel in the plasma membrane of rye roots have been presented previously (White, 1993, 1996).

Results

The maxi cation channel in the plasma membrane of rye roots is permeable to both monovalent and divalent cations (White, 1993, 1997). Physiologically, the most important of these will be the monovalent cations K^+ and Na^+, and the essential divalent cations Ca^{2+}, Mg^{2+} and Mn^{2+}. The selectivity sequence for the maxi cation channel based on unitary conductances measured in the presence of symmetrical 100 mM cation chloride differed from that based on relative permeabilities estimated using the Goldman-Hodgkin-Katz (GHK) equation in the presence of (*cis:trans*) 100 mM cation chloride: 100 mM KCl (White, 1993). It is, therefore, inappropriate to model cation permeation through the channel using the GHK current equation, since it cannot describe this phenomenon (Hille, 1992). In addition, apparent relative permeabilities (as defined by the GHK equation) varied with concentration under equimolar bi-ionic conditions and with the concentration of a slowly permeating cation applied to one side of the channel in the presence of a constant K^+ concentration gradient (White, 1997). The former observation cannot be accommodated by permeation models based on ions traversing a rigid free-energy profile containing only a single ion (Hille, 1992). Indeed, models presuming a single binding site (whether in a rigid pore or a dynamic pore as described by Hansen, Keunecke & Blunck, 1997) may be structurally ill conceived: It is expected that the selectivity filter of many ion channels will contain several ions simultaneously, as was recently demonstrated for the KcsA channel from *Streptomyces lividans* (Doyle et al., 1998). It is likely that the permeation properties of the maxi cation channel mentioned above reflect complex interactions between cations within the pore of the channel. They can be accommodated by a theoretical pore structure that can be occupied simultaneously by more than one cation.

In this paper the pore of the maxi cation channel has been modeled using the simplest pore structure that can accommodate two ions simultaneously. This has three energy barriers and two ion-binding sites (3B2S model). Single-file permeation was assumed, as well as double cation occupancy. Ion-ion repulsion and surface potential effects were included explicitly. The proposed 3B2S model adequately accounted for the diverse phenomena associated with cation permeation through this channel. Data were obtained throughout the voltage range over which the unitary current through the channel could be reliably estimated under a wide variety of ionic conditions (e.g., Figs. 1 to 11). Parameters were fitted to

Table 2. Estimated parameters for the 3B2S double ion residency model for K^+, Na^+, Ca^{2+} and Ba^{2+} permeation through the maxi cation channel in the plasma membrane of rye roots

	K^+	Na^+	Ca^{2+}	Ba^{2+}
G1	3.64 (0.082)	4.23 (0.107)	4.38 (0.146)	3.61 (0.180)
G2	3.07 (0.100)	0.34 *	−1.40 *	0.96 (0.239)
G3	4.15 (0.057)	5.01 (0.075)	3.99 (0.179)	3.65 (0.195)
U1	2.52 *	−5.11 (0.181)	−9.40 (0.237)	−8.77 (0.321)
U2	−5.48 (0.079)	−5.30 (0.144)	−8.87 (0.277)	−9.50 (0.255)
A			0.29 (0.036)	
D1			0.09 (0.010)	
D2			0.32 (0.023)	
D3			0.56 (0.017)	
D4			0.57	
D5			0.80 (0.009)	
R_{scis}			18.60 (0.60)	
R_{strans}			27.00 (1.72)	

Parameters were estimated from *I/V* data collected across a wide variety of ionic conditions. The total number of observations was 1460 and the residual sum of squares was 14685. Standard errors of parameter estimates are shown in parenthesis. The parameter D4 was fixed (to its optimal value) in relation to D3 during the fitting process. This was required because D4 could not be estimated with any precision, and it was necessary to constrain the model to prevent inappropriate estimates. All other parameters were free to vary. Three parameters had large standard errors and are marked with an asterisk. These parameters are estimated with low precision, but reliable estimates of their standard errors are not available. The parameters G1, G2, G3, U1 and U2 are expressed in (dimensionless) multiples of RT. The solution reference state is 55.5 M.

the complete set of 1460 datapoints obtained under 77 different ionic conditions (Table 2). Although better fits to *I/V* data for individual experiments could be obtained with slightly different parameter values, the estimates given here offer a composite description of the pore structure of the maxi cation channel.

Pore Structure of the Channel

The 3B2S model which best fitted the data suggested that the free energy profile for the channel was conspicuously asymmetrical and that the free energy profile for K^+ was distinctly different from those for Na^+, Ca^{2+} and Ba^{2+} (Table 2). For K^+ the free energy peaks were all of a similar magnitude, but for other cations the central energy peak (G2) was lower than the peaks at the ends of the pore (G1 and G3). The peaks at the ends of the pore were of a similar magnitude and differed little between cations. The magnitudes of the central energy peaks for Na^+, Ca^{2+} and Ba^{2+} were similar and, although they were not estimated very precisely, they were clearly much lower than that for K^+. A similar inability to estimate precisely the height of the central peak was experienced in describing monovalent cation permeation through a K^+ channel in the plasma membrane of rye roots using a 3B2S model (White & Ridout, 1995). In the present study, the depth of the *cis* free energy well (U1) for K^+ was also estimated poorly, but was clearly much higher than the *trans* free energy well (U2). For other cations, U1 was similar in magnitude to U2. Both U1 and U2 were higher for monovalent cations than for divalent cations. The free energy values for U1 decreased in the order $K^+ > Na^+ > Ba^{2+} \simeq Ca^{2+}$ and the free energy values for U2 decreased in the order $Na^+ = K^+ > Ca^{2+} \simeq Ba^{2+}$. The affinity of the binding sites was not great, but divalent cations had a higher affinity than monovalent cations. The dissociation binding constant (K_d) of the binding-sites for divalent cations in an unoccupied pore was between 4 to 9 mM, but the K_d for monovalent cations was at least 25-fold higher. In addition, the model suggested significant repulsion between cations within the pore, which would increase the free-energy of the unoccupied binding site in an occupied pore by 1.16 to 4.64 RT units, depending upon the valency of the interacting cations. Significant surface charge in both the external (*cis;* 0.0009 e/Å^2) and cytoplasmic (*trans;* 0.0004 e/Å^2) vestibules of the channel was also suggested.

Permeation of Monovalent Cations

The data obtained in the presence of both symmetrical (Fig. 1*A* and *B*) and asymmetrical (Fig. 2*A*) KCl solutions were described adequately by the proposed 3B2S model. A slight deviation between the observed and modeled *I/V* relationship was observed in the presence of (*cis:trans*) 1:100 mM KCl, under which conditions the observed E_{rev} was more negative than the Nernst potential for K^+. This was also noted by White (1993). The simplest explanation of this is that the actual K^+ concentration in the *cis* solution was greater than 1 mM. This may be a consequence of either incomplete perfusion of the *cis* chamber and/or K^+ leakage from the 3 M KCl salt bridges. The proposed 3B2S model also adequately described the *I/V* relationships obtained in the presence of symmetrical NaCl solutions (Fig. 3*A* and *B*), although at NaCl concentrations of 100 mM and below, the modeled currents at positive voltages were slightly lower than the measured currents.

The proposed 3B2S model predicted *I/V* relationships which closely approximated those measured in solutions containing equimolar (*cis:trans*) NaCl:KCl at most cation concentrations (Fig. 4*A*). The shape of the *I/V* relationship observed in the presence of 1 mM NaCl:KCl deviated from the modeled *I/V* curve resulting in a marked difference between the observed and the fitted E_{rev} (Fig. 4*B*), but, since the slope of the *I/V* relationship is very flat, small changes in slope have a large

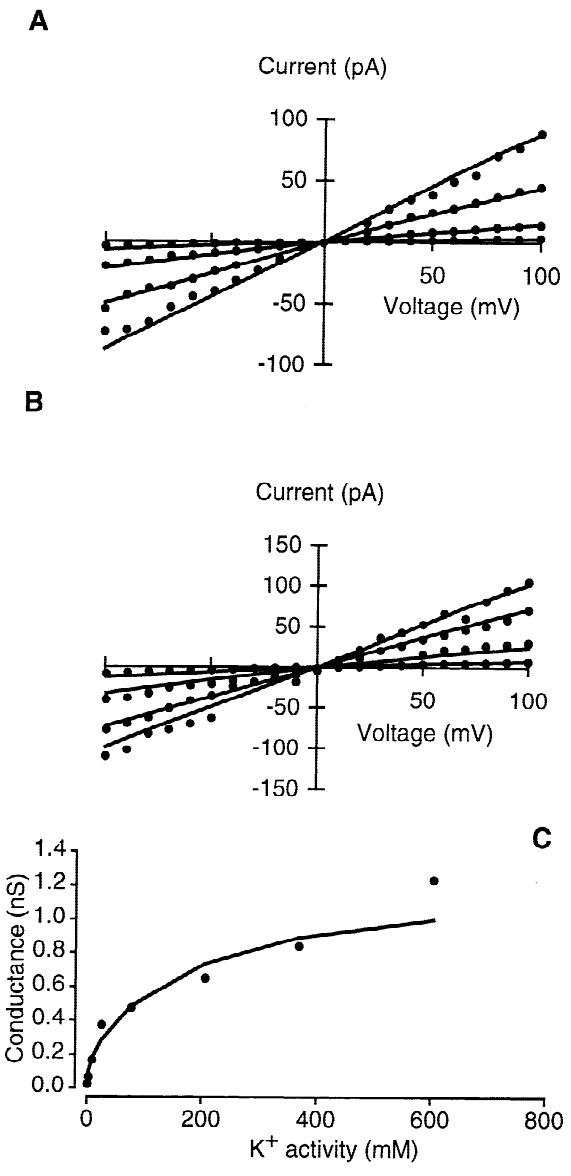

Fig. 1. (*A* and *B*) Unitary-current *vs.* voltage relationships and (*C*) unitary-conductance *vs.* K^+ activity relationship for the maxi cation channel from the plasma membrane of rye roots assayed in a planar PE bilayer in the presence of symmetrical KCl solutions. Solutions contained (*A*) 1, 10, 100 and 579 mM KCl, and (*B*) 3, 30, 300 and 1000 mM KCl. Unitary conductance was determined between ±30 mV. The curves are derived from a theoretical 3B2S model with the parameters shown in Table 2.

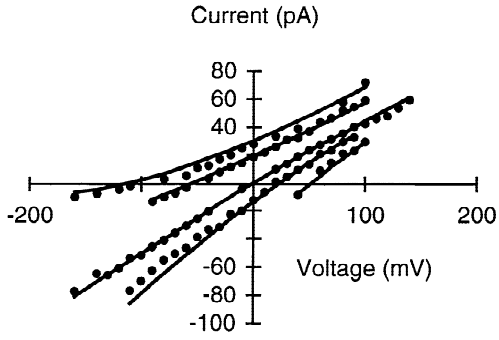

Fig. 2. Unitary-current *vs.* voltage relationships for the maxi cation channel from the plasma membrane of rye roots assayed in a planar PE bilayer in the presence of asymmetrical (*trans:cis*) 100:1, 100:10, 100:280, 100:1000 mM KCl. For clarity data for 100:603 and 100:364 mM KCl were excluded from the figure. The curves are derived from a theoretical 3B2S model with the parameters shown in Table 2.

effect on the estimated E_{rev}. In addition, comparing the observed and fitted E_{rev} is a sensitive test of the model, since the regression was based only on deviations from the observed current. As the concentrations of NaCl and KCl were increased symmetrically from 1 mM to 30 mM the observed E_{rev} became more negative, and the E_{rev} at 30 mM NaCl:KCl was approximated by the model. Furthermore, as the concentrations of NaCl and KCl were increased above 30 mM, the E_{rev} predicted by the model continued to approximate the observed E_{rev} as it became more positive with increasing ionic concentrations.

Permeation of Divalent Cations

The 3B2S model proposed for Ba^{2+} predicted an *I/V* relationship in the presence of symmetrical 100 mM $BaCl_2$ which rectified at extreme voltages, both negative and positive. This contrasts with previous representations of this *I/V* relationship as an ohmic, linear *I/V* relationship (*compare* Fig. 5 with White, 1993). The proposed 3B2S model also predicted *I/V* relationships rectifying at high positive and negative voltages in the presence of (*cis:trans*) 100 mM $BaCl_2$:KCl. The recorded data appear consistent with this interpretation, and the predicted E_{rev} of 12.7 mV in the presence of 100 mM $BaCl_2$:KCl is similar to the value of 10 mV estimated from a linear interpolation between data at −60 and +50 mV by White (1993).

When 100 mM KCl was present on both sides of the channel, increasing the Ba^{2+} concentration in the *cis* (extracellular) solution resulted in a voltage-dependent decrease in currents at both negative and positive voltages and an apparent shift in E_{rev} to more positive values with increasing Ba^{2+} concentrations (Fig. 6*A*). By contrast, an equivalent increase in Ba^{2+} concentration in the *trans* (cytoplasmic) solution resulted only in a slight voltage-dependent decrease in current at negative voltages and a negative shift in E_{rev} (Fig. 2*B*). These phenomena were faithfully described by the proposed 3B2S model. The inhibition of the K^+ current through this channel by Ba^{2+} appears to be a direct consequence of slow Ba^{2+} permeation.

The 3B2S model proposed for Ca^{2+} permeation fitted the data obtained in the presence of symmetrical

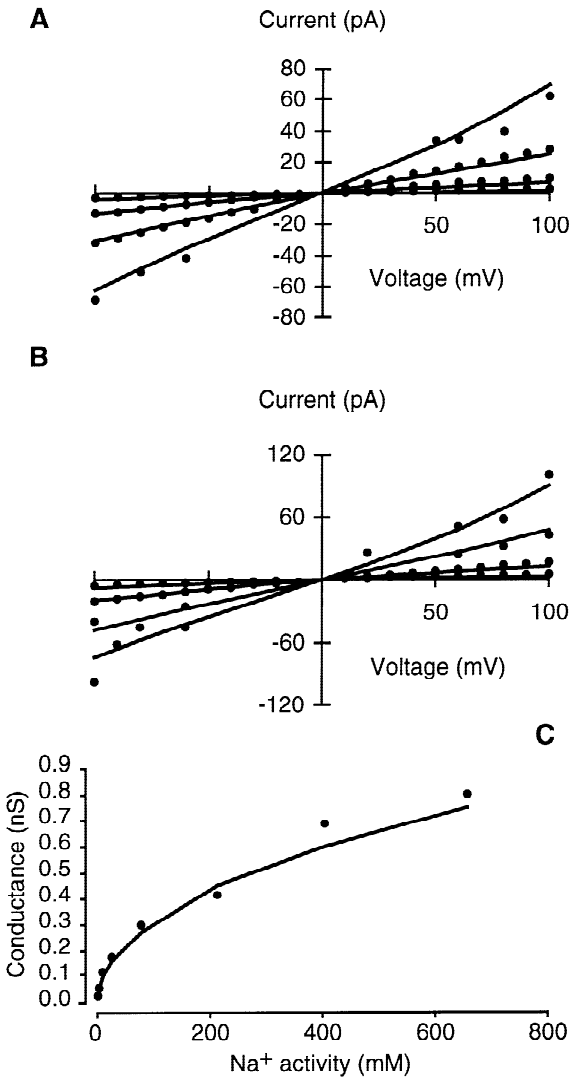

Fig. 3. (*A* and *B*) Unitary-current *vs.* voltage relationships and (*C*) unitary-conductance *vs.* Na^+ activity relationship for the maxi cation channel from the plasma membrane of rye roots assayed in a planar PE bilayer in the presence of symmetrical NaCl solutions. Solutions contained (*A*) 1, 10, 100 and 600 mM NaCl, and (*B*) 3, 30, 300 and 1000 mM NaCl. Unitary conductance was determined between ±60 mV. The curves are derived from a theoretical 3B2S model with the parameters shown in Table 2.

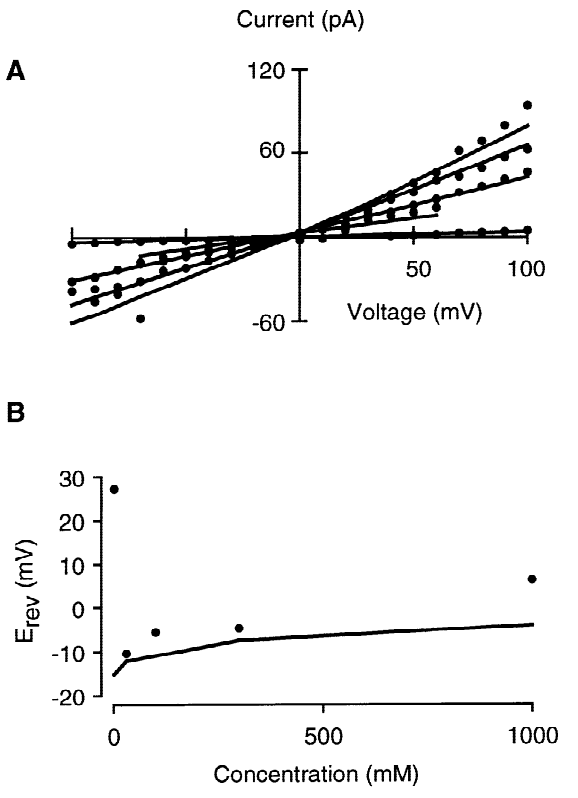

Fig. 4. (*A*) Unitary-current *vs.* voltage relationships and (*B*) the relationship between E_{rev} and monovalent ion concentration for the maxi cation channel from the plasma membrane of rye roots assayed in a planar PE bilayer in the presence of equimolar (*cis:trans*) Na^+:K^+. The monovalent cation concentrations were 1, 30, 100, 300 and 1000 mM. The curves are derived from a theoretical 3B2S model with the parameters shown in Table 2.

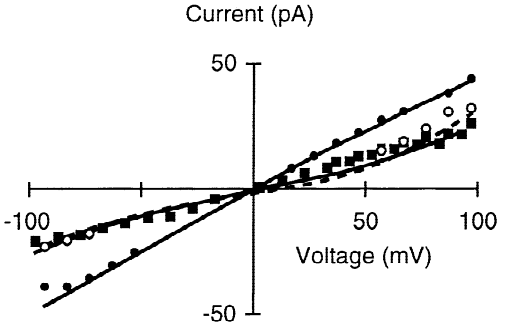

Fig. 5. Unitary-current *vs.* voltage relationships for the maxi cation channel from the plasma membrane of rye roots assayed in a planar PE bilayer in the presence of symmetrical 100 mM KCl (●), symmetrical 100 mM $BaCl_2$ (■) and (*cis:trans*) 100 mM $BaCl_2$: 100 mM KCl (○). The curves are derived from a theoretical 3B2S model with the parameters shown in Table 2.

$CaCl_2$ solutions at concentrations above 30 mM (Fig. 7). However, in solutions containing 30 mM $CaCl_2$ and below, the modeled *I/V* relationships exhibited considerable rectification and the currents predicted by the model were greater than those observed experimentally at extreme voltages. The model fitted the observed relationship between unitary conductance (determined between +30 and −30 mV) and Ca^{2+} activity adequately, showing a high conductance at low Ca^{2+} activities and rising almost linearly between 12 and 170 mM with a gradient of 0.98 pS/mM (Fig. 7*C*).

The proposed 3B2S model predicted a rectifying *I/V* relationship in the presence of (*cis:trans*) 100 mM $CaCl_2$:$BaCl_2$ (Fig. 8). The *I/V* relationship determined experimentally differed from this interpretation by ap-

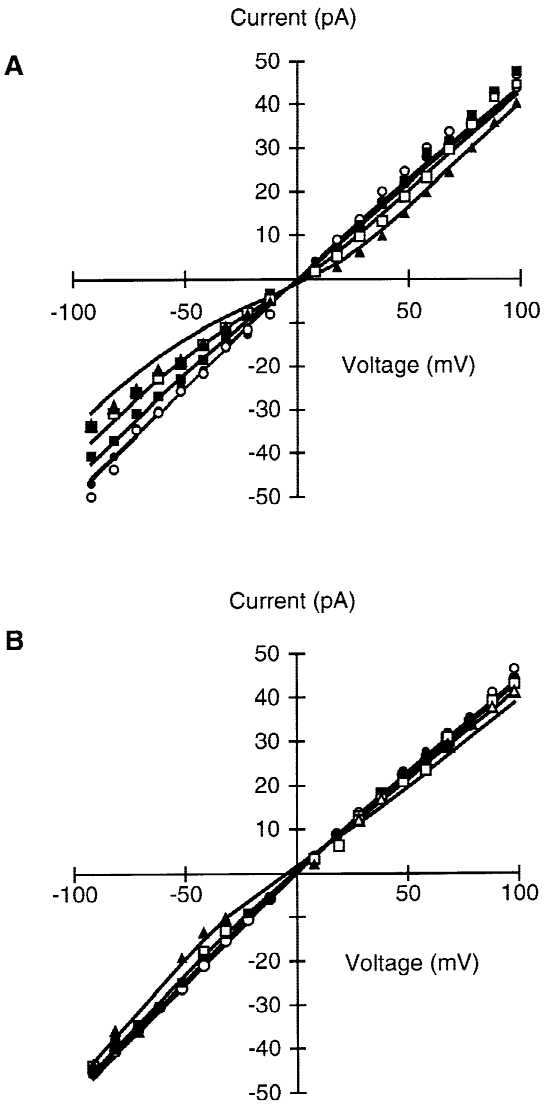

Fig. 6. The effect of Ba^{2+} in (*A*) the *cis* and (*B*) the *trans* solution on the unitary-current *vs.* voltage relationships for the maxi cation channel from the plasma membrane of rye roots assayed in a planar PE bilayer in the presence of symmetrical 100 mM KCl. Data in the absence of Ba^{2+} (●) and for Ba^{2+} concentrations of 0.1 (○), 1 (■), 3 (□) and 10 mM (▲) are shown. Data for Ba^{2+} concentrations of 0.03 and 0.3 mM have been excluded from the figure for clarity. The curves are derived from a theoretical 3B2S model with the parameters shown in Table 2.

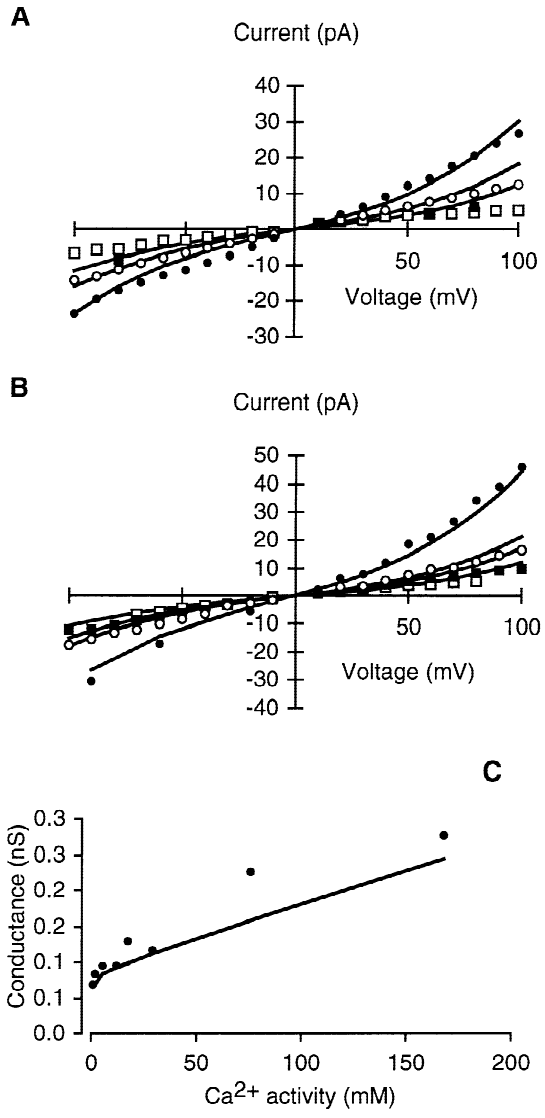

Fig. 7. (*A* and *B*) Unitary-current *vs.* voltage relationships and (*C*) unitary-conductance *vs.* Ca^{+} activity relationship for the maxi cation channel from the plasma membrane of rye roots assayed in a planar PE bilayer in the presence of symmetrical $CaCl_2$ solutions. Solutions contained (*A*) 1, 10, 50 and 300 mM $CaCl_2$, and (*B*) 5, 30, 100 and 600 mM $CaCl_2$. Unitary conductance was determined between ±30 mV. The curves are derived from a theoretical 3B2S model with the parameters shown in Table 2.

pearing linear (White, 1993). An E_{rev} of −4.7 mV was predicted by the model, which agrees with the value of −5 mV suggested by White (1993) based on a linear interpolation between data at −70 and +30 mV.

In general, the proposed 3B2S model successfully fitted the data obtained when channel currents were measured in the presence of equimolar (*cis:trans*) $CaCl_2$:KCl concentrations between 3 and 300 mM (Fig. 9*A*). However, the modeled currents at high negative voltages were slightly greater than the currents observed at cation concentrations of 10 mM and below. The E_{rev} observed under equimolar (*cis:trans*) $CaCl_2$:KCl conditions decreased with increasing cation concentration (Fig. 9*B*). The E_{rev} predicted by the proposed 3B2S model followed this trend, although some discrepancies between the predicted and observed E_{rev} were apparent.

In the presence of 100 mM KCl on both sides of the channel, the addition of submillimolar concentrations of Ca^{2+} to the *cis* solution appeared to increase the unitary current at negative voltages (Fig. 10*A*). This was not

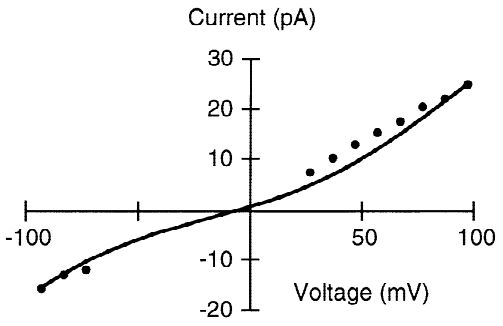

Fig. 8. Unitary-current *vs.* voltage relationships for the maxi cation channel from the plasma membrane of rye roots assayed in a planar PE bilayer in the presence of (*cis:trans*) 100 mM $CaCl_2$: 100 mM $BaCl_2$. The curve is derived from a theoretical 3B2S model with the parameters shown in Table 2.

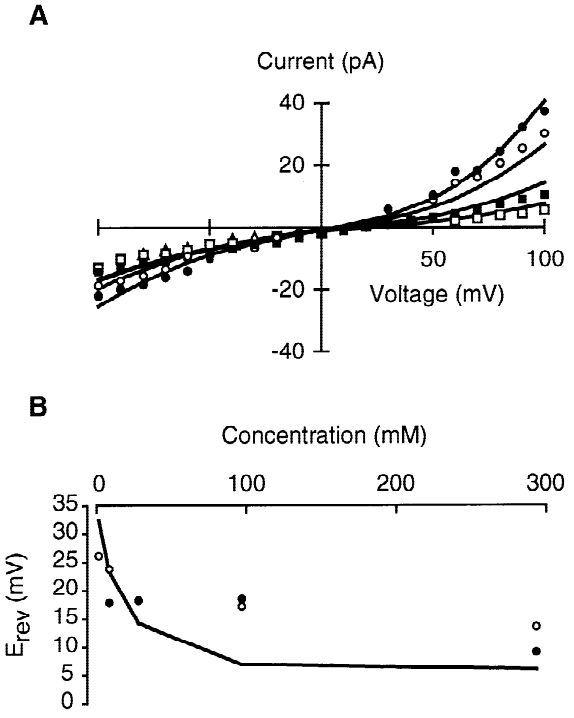

Fig. 9. (*A*) Unitary-current *vs.* voltage relationships for the maxi cation channel from the plasma membrane of rye roots assayed in a planar PE bilayer in the presence of equimolar (*cis:trans*) $CaCl_2$:KCl. The salt concentrations were 3, 10, 30, 100 and 300 mM. (*B*) The relationship between E_{rev} and cation concentration. Data were (●) determined from the *I/V* relationships shown in panel *A* or (○) provided by White (1997). The curves are derived from a theoretical 3B2S model with the parameters shown in Table 2.

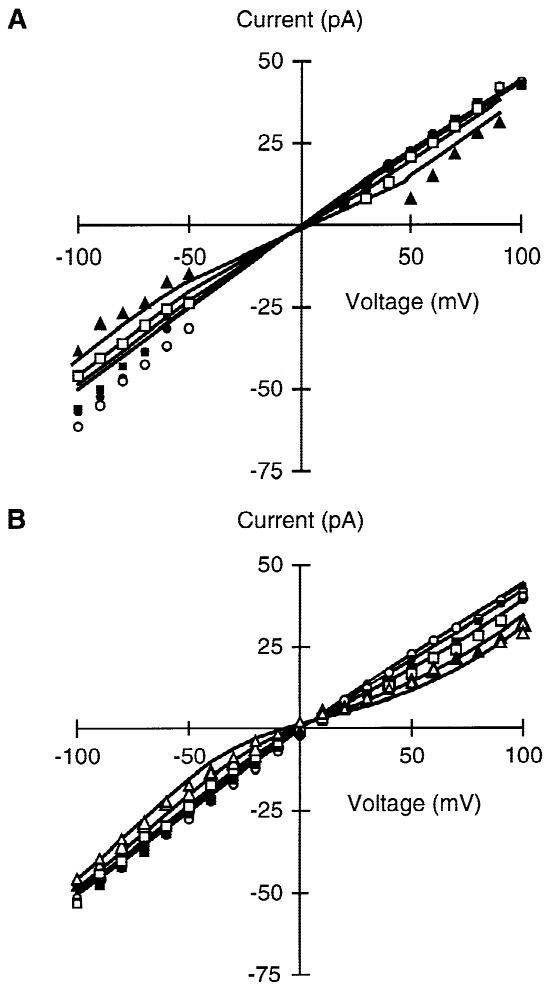

Fig. 10. The effect of Ca^{2+} in (*A*) the *cis* and (*B*) the *trans* solution on the unitary-current *vs.* voltage relationships for the maxi cation channel from the plasma membrane of rye roots assayed in a planar PE bilayer in the presence of symmetrical 100 mM KCl. Data in the absence of Ca^{2+} (●) and for Ca^{2+} concentrations of 0.1 (○), 1 (■), 3 (□), 10 mM (▲) and 30 mM (△) are shown. Data for Ca^{2+} concentrations of 0.03 and 0.3 mM have been excluded from the figure for clarity. The curves are derived from a theoretical 3B2S model with the parameters shown in Table 2.

described by the proposed 3B2S model and the origin of this phenomenon is unknown. Increasing the Ca^{2+} concentration in the *cis* solution from 1 mM progressively reduced the unitary-current at both negative and positive voltages, but had little effect on E_{rev}. This was accurately described by the proposed 3B2S model. When micromolar Ca^{2+} was added to the *trans* solution, no marked increase in current was observed at any voltage (Fig. 10*B*). As the Ca^{2+} concentration was increased into the millimolar range the unitary currents at both negative and positive voltages were progressively reduced and the E_{rev} became increasingly more negative. These observations were also accurately described by the proposed 3B2S model.

Under ionic conditions which approximate those commonly encountered physiologically with 100 mM KCl plus contaminant Ca^{2+} on the *trans* (cytoplasmic) side of the channel and 1 mM KCl on the *cis* (extracel-

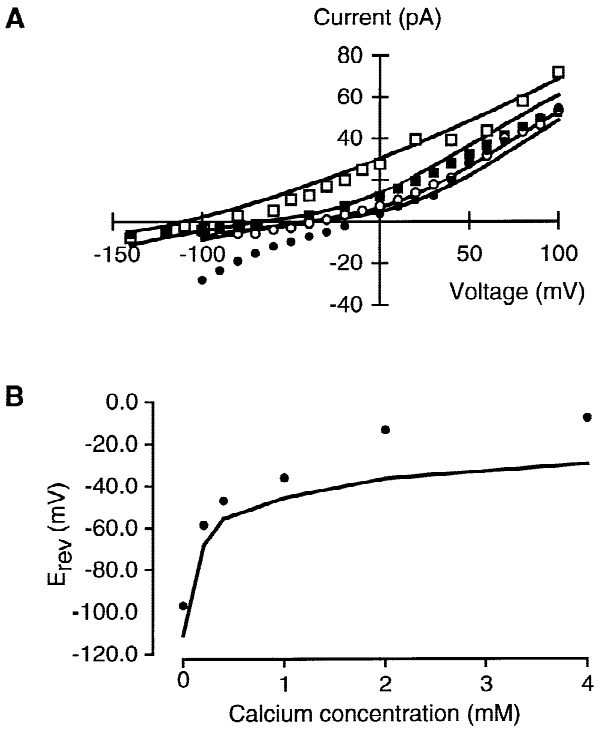

Fig. 11. The effect of Ca^{2+} in the *cis* solution on (*A*) the unitary-current *vs.* voltage relationships and (*B*) the E_{rev} for the maxi cation channel from the plasma membrane of rye roots assayed in a planar PE bilayer in the presence of asymmetrical (*cis:trans*) 1:100 mM KCl. Data in the absence of Ca^{2+} (□) and for Ca^{2+} concentrations of 0.2 (■), 1 (○) and 2 mM (●) are shown. Data at a Ca^{2+} concentration of 0.5 mM have been excluded from panel *A* for clarity and the E_{rev} at 4 mM Ca^{2+} is from White (1997). The curves are derived from a theoretical 3B2S model with the parameters shown in Table 2.

lular) side of the channel (White, 1993; Marschner, 1995), increasing the Ca^{2+} concentration in the *cis* solution shifted the E_{rev} to more positive voltages, presumably by increasing the Ca^{2+} current from the *cis* to the *trans* chamber (Fig. 11*A*). The proposed 3B2S model described the various *I/V* relationships observed with increasing Ca^{2+} concentrations up to and including 1 mM. However, when 2 mM Ca^{2+} was present in the *cis* solution, the observed unitary-current exhibited a pronounced rectification at negative voltages and was far greater than that described by the 3B2S model. Such rectification was not predicted by the model even when the Ca^{2+} concentration in the *cis* solution was increased to 4 mM. The proposed 3B2S model described the shift in E_{rev} to more positive voltages as the Ca^{2+} concentration in the *cis* solution was increased (Fig. 11*B*). However, the predicted E_{rev} was systematically more negative than the observed E_{rev}. In these experiments the E_{rev} estimated in the presence of (*cis:trans*) 1:100 mM KCl was 97 mV. Assuming negligible Cl^- permeability, this corresponds to a K^+ activity of 1.65 mM and a K^+ concentration of 1.73 mM. However, using this value for the K^+ concentration in the *cis* solution resulted in a decrease of less than 1 mV in the E_{rev} predicted by the proposed 3B2S model.

Discussion

Adequacy of the Proposed 3B2S Model

In general, the proposed 3B2S model fitted the experimental data well, but two exceptions can be noted initially. First, the proposed 3B2S model failed to describe the shape of the *I/V* relationship and the E_{rev} when the channel was assayed in the presence of bi-ionic (*cis:trans*) 1 mM NaCl:KCl (Fig. 4). However, this might be an artefact resulting from difficulties in attaining low cation concentrations in experiments. Second, the model failed to describe the rectifying current observed at negative voltages in the presence of (*cis:trans*) 1:100 mM KCl plus 2 mM $CaCl_2$ (Fig. 11). Neither could the model reproduce this effect when the Ca^{2+} concentration in the *cis* solution was increased to 4 mM.

The proposed 3B2S model accounted for: (i) the diverse *I/V* relationships obtained for the maxi cation channel over a wide range of concentrations in both single salt and mixed solutions; (ii) the non-Michaelian unitary-conductance *vs.* ionic activity relationships for K^+, Na^+ and Ca^{2+} when assayed under symmetrical ionic conditions (Figs. 1*C*, 3*C* and 7*C*); (iii) the changes in E_{rev} recorded under bi-ionic conditions as cation concentrations were increased from 30 to 1000 mM NaCl:KCl (Fig. 4*B*) or 3 to 300 mM $CaCl_2$:KCl (Fig. 9*B*), and the E_{rev} recorded in bi-ionic 100 mM (*cis:trans*) $BaCl_2$:KCl (Fig. 5) and $CaCl_2$:$BaCl_2$ (Fig. 8); (iv) the diverse *I/V* relationships observed when either Ba^{2+} (Fig. 6) or Ca^{2+} (Fig. 10) were added to the *cis* or *trans* chambers in the presence of symmetrical 100 mM KCl; (v) the changing *I/V* relationships and E_{rev} observed in the presence of (*cis:trans*) 1:100 mM KCl as the concentration of Ca^{2+} in the *cis* compartment was increased to 1 mM (Fig. 11). Indeed, the proposed 3B2S model fitted the majority of experimental data and adequately described cation permeation through the pore of the maxi cation channel.

Although the permeation of cations through many channels has been modeled as movement through a rigid free-energy profile that can contain several interacting cations simultaneously (Hille, 1992), several alternative models have been used to describe permeation through cation channels in plant cell membranes. Recently Gradmann and coworkers employed single binding site models to describe Ca^{2+} and K^+ permeation through two cation channels in the tonoplast of plant cells (Gradmann, Johannes & Hansen, 1997; Allen, Sanders & Gradmann, 1998). They considered two types of model: a simple rigid-pore (2B1S) model and a dynamic-pore

model. The dynamic-pore model incorporated a selectivity filter in which the binding site alternated its orientation between one side of the membrane and the other within a fraction of the electrical distance and in a rate limiting fashion. The dynamic-pore model was slightly superior to the 2B1S model in describing *I/V* data from both channels (Gradmann et al., 1997; Allen et al., 1998). However, structural studies suggest that the selectivity filter of a channel may be occupied by several cations simultaneously (Doyle et al., 1998), and provide no evidence for conformational changes in the selectivity filter during permeation. In addition, several properties of the maxi cation channel cannot be described by simple single binding site models. For example, the 2B1S model (Hille, 1992) cannot account for changes in E_{rev} under bi-ionic conditions as the cation activities on both sides of the membrane are raised proportionally (Figs. 4 and 9) and the dynamic-pore model (Gradmann et al., 1997; Allen et al., 1998) predicts supralinear *I/V* relationships (e.g., current saturation at extreme voltages) and trans-inhibition (a reduction in current when the concentration of a permeant ion is increased on the opposite side of the membrane), which do not occur in the data presented here.

Ultimately, it might be useful to consider more complex models for cation permeation, such as those involving solutions to the Poisson-Nernst-Planck (PNP) equations (Eisenberg, 1996; Nonner, Chen & Eisenberg, 1998; Nonner & Eisenberg, 1998). The PNP equations provide a self-consistent theory for electrodiffusion and promise to yield detailed information about the permanent charge profile within the channel pore. Unfortunately, the application of such models is limited at present, not only by the requirement for great computational power but also by the paucity of structural information regarding pore dimensions. Nevertheless, it would be interesting, eventually, to compare the structural features of the pore suggested by the 3B2S model described here with those suggested by models based on the PNP equations.

Inferences for the Structure of the Channel Pore

Several inferences can be made from the proposed 3B2S model regarding the structure of the pore of the maxi cation channel. First, the pore appears to be asymmetrical, which is not uncommon for any ion channel (Hille, 1992; Aidley & Stanfield, 1995). This produces the asymmetrical *I/V* relationships observed under symmetrical ionic conditions (Figs. 1, 3, 5 and 7) and gives rise to the side-dependent effects of Ba^{2+} and Ca^{2+} on the *I/V* relationships recorded in the presence of symmetrical 100 mM KCl (Figs. 6 and 10). Second, the binding-sites within the pore have a greater affinity for divalent cations than for monovalent cations. This characteristic has been predicted for several Ca^{2+} channels in the membranes of animal cells (Hille, 1992; Tikhonov & Magazanik, 1998). Both selectivity and blockade of the channel can, therefore, be generated by occupancy of the pore. In the absence of divalent cations the maxi cation channel is highly permeable to monovalent cations. However, when divalent cations are present, they occupy the pore preferentially and restrict the permeation of monovalent cations. Third, the channel exhibits low selectivity between cations. This occurs because the affinity for even divalent cations is minimal and the dominant free energy peaks for all cations are comparable (Hille & Schwarz, 1978). The increasing permeability to Na^+ and Ca^{2+} relative to K^+ with increasing cation concentration (Figs. 4 and 9) results predominantly from differences in the height of the central energy peak (G2) between Na^+ and Ca^{2+}, and K^+. The free-energy profile in the pore region adjacent to the *cis* (extracellular) solution appeared to be the primary determinant of cation selectivity. A major structural component conferring selectivity between cations appears to be the diameter of the pore. Larger cations such as TEA^+ do not permeate (White, 1993). Fourth, there is considerable surface charge at the mouths of the channel pore. This will serve to concentrate cations in the pore vestibules and thereby increase cation fluxes at low concentrations in the bulk solution. This is illustrated by the high unitary conductances recorded in the presence of low KCl, NaCl and $CaCl_2$ concentrations (Figs. 1, 3 and 7). The presence of surface charge would also decrease anion concentrations in the vestibules, thereby restricting their entry to the pore. This appears to be a general characteristic of cation channels (Hille, 1992; Chilcott et al., 1995; Aidley & Stanfield, 1996; Doyle et al., 1998). It would be worth attempting to verify this supposition independently for the maxi cation channel.

Utility of the Proposed Model for Predictive Purposes

A Ca^{2+} flux across the plasma membrane entering the cytoplasm of a root cell, and the consequent increase in cytosolic Ca^{2+} concentration, has been implicated as a signal in a variety of physiological processes (reviewed by White, 1998*a*). It has been suggested that depolarization-activated, Ca^{2+}-permeable channels, such as the maxi cation channel, mediate this Ca^{2+} influx. The plasma membrane of the root cell can be viewed as a dynamic system of ion transport mechanisms coupled via the membrane voltage. Since the maxi cation channel is regulated by membrane voltage it is an integral component of this system. Its activity will not only be influenced by membrane voltage but, through the flux it mediates, it will also influence the membrane voltage.

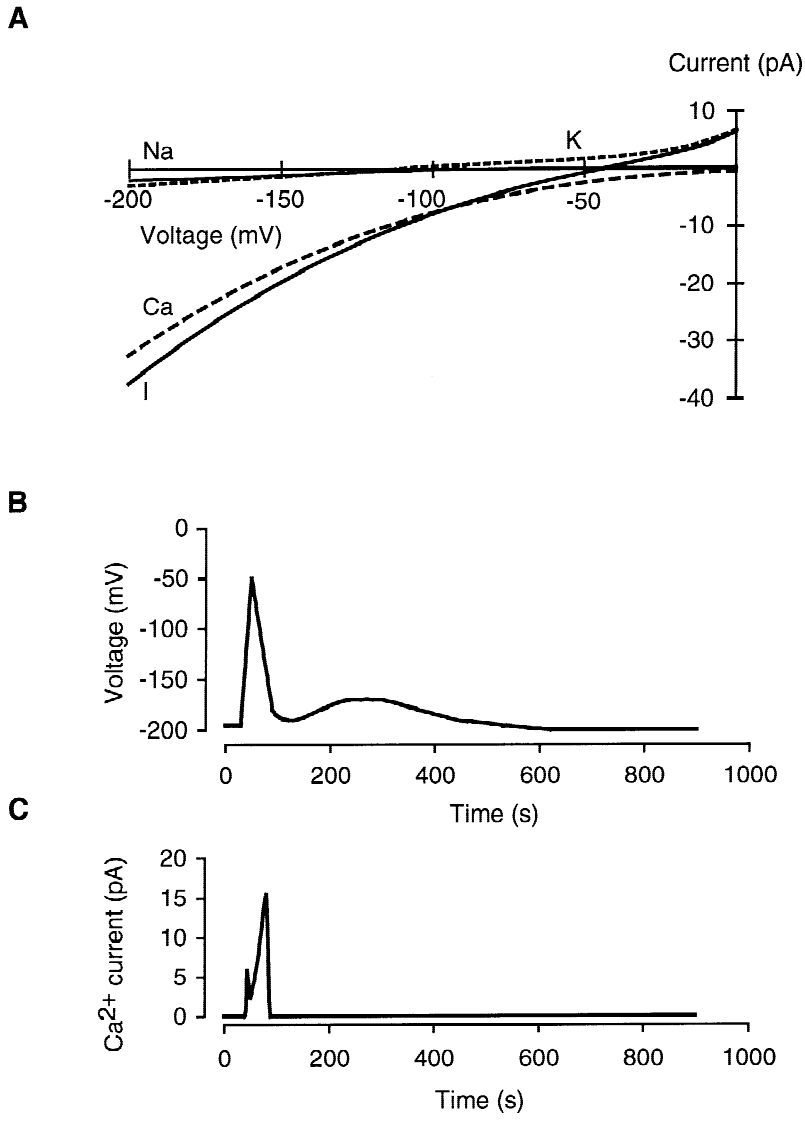

Fig. 12. (*A*) The predicted voltage-dependence of the unitary current (—) and net K^+ (----), Na^+ (—) and Ca^{2+} (– – – –) currents through the maxi cation channel in the plasma membrane of rye roots determined under physiological conditions at 20°C. The extracellular solution contained 1 mM concentrations of K^+, Na^+ and Ca^{2+}. The cytoplasmic K^+, Na^+ and Ca^{2+} activities were 71.5 mM, 3.5 mM, and 100 nM, respectively. The E_{rev} was −43.0 mV. (*B*) Typical slow action potential (SAP) induced in cucumber roots after 30 *sec* by rapid cooling (20°C min^{-1}) from 23°C to 18°C followed by rewarming (data taken from Minorsky & Spanswick, 1989). (*C*) The mean Ca^{2+} influx through a single maxi cation channel during the SAP shown in panel *B*. The Ca^{2+} influx was calculated as the probability of the channel being active multiplied by the net Ca^{2+} current through the channel.

Recently there has been much interest in modeling the electrocoupling of ion transport mechanisms at the plasma membrane, in particular in relation to osmotic adjustment (Gradmann, Blatt & Thiel, 1993; Gradmann & Buschmann, 1997; Gradmann & Hoffstadt, 1998). Of equal interest, perhaps, is the electrocoupling which occurs during cell signaling. The components required to describe the effects of electrocoupling on an ion channel in the plasma membrane include the voltage-dependence of channel kinetics, the ionic current mediated by the channel, and, for a physiological interpretation, the individual ion fluxes occurring. A model for the permeation of monovalent and divalent cations through the maxi cation channel in the plasma membrane of rye roots is presented in this paper, from which both net current and the fluxes of individual ions can be predicted. These data can be used, together with data on the kinetics of the maxi cation channel (White, 1993, 1997), as primary inputs to an electrocoupling model enabling a study of the effects of, for example, environmental stimuli on membrane voltage and Ca^{2+} fluxes.

Calcium Influx Upon Transient Root Chilling: A Prediction

Cooling plant roots briefly to low, non-freezing temperatures elicits a perturbation in cell membrane potential termed a slow action potential (SAP; Minorsky, 1989). The SAP consists of a membrane depolarization, followed by subsequent repolarization and restoration of the resting potential (Fig. 12*B*). It is thought that depolarization-activated Ca^{2+}-permeable channels allow Ca^{2+} influx during the SAP and that the consequent rise in cytoplasmic Ca^{2+} concentration initiates an acclimatory response (White, 1998*a*). The Ca^{2+} influx during a SAP

through a single maxi cation channel in the plasma membrane of a root cell can be estimated by combining the 3B2S model described here with a simplified kinetic model of the maxi cation channel.

The kinetics of the maxi cation channel are dominated by inactivation at extreme voltages (White, 1993). For simplicity, it was assumed that the open probability of the active channel was unity. The kinetic scheme is:

$$\text{Active} \underset{k_{-1}}{\overset{k_1}{\rightleftarrows}} \text{Inactive}$$

The rate-constants for both channel inactivation (k_1; sec^{-1}) and channel activation (k_{-1}; sec^{-1}) are voltage-dependent and can be approximated by the equations:

$$k_1 = e^{(-20.72 - (V * 0.173))}$$

$$k_1 = e^{(13.82 + (V * 0.210))}$$

The equation for k_1 was determined from the time constants for channel inactivation ($\tau_c = 1/k_1$) presented by White (1993), and that for k_{-1} was estimated by fitting the voltage-ramp experiments presented for the maxi cation channel by White (1998*a*). It was assumed that the voltage dependence of both k_1 and k_{-1} varied in parallel with changes in the E_{rev} of the current mediated by the channel (*cf.* White 1993), and V is defined as the voltage displacement from E_{rev}.

The probability of finding an active channel (P_a) at time (t) was determined from the relationships (Gray, 1987):

$$P_a(t) = P_a(\infty) + [P_a(0) - P_a(\infty)]e^{-t/\tau}$$

$$P_a(\infty) = k_{-1}/(k_1 + k_{-1})$$

and

$$\tau = 1/(k_1 + k_{-1})$$

The influence of voltage on the net currents and ionic fluxes was determined at the appropriate temperature under physiological ionic conditions for K^+, Na^+ and Ca^{2+} using the proposed 3B2S model (Fig. 12*A*). The activities of K^+, Na^+ and Ca^{2+} used for the predictions were 0.904 mM, 0.930 mM and 0.696 mM in the extracellular solution and 71.5 mM, 3.5 mM, and 100 nM in the cytoplasm, respectively. It can be noted that the proposed 3B2S model adequately fitted the *I/V* relationship obtained in the presence of (*cis:trans*) concentrations of 1 mM $CaCl_2$ plus 1 mM KCl: 100 mM KCl (Fig. 11) and although there was a discrepancy between the observed and fitted *I/V* relationships when assayed in the presence of (*cis:trans*) 1 mM NaCl: 1 mM KCl (Fig. 4), the latter could be a consequence of experimental difficulties in attaining low cation concentrations. The predicted E_{rev} under physiological ionic conditions varied from −42.5 mV at 18°C to −43.6 mV at 23°C. The net Ca^{2+} influx was calculated by multiplying P_a with the predicted Ca^{2+} flux through an individual channel at the appropriate voltage and temperature (Fig. 12*C*).

The predicted Ca^{2+} influx through the maxi cation channel during a SAP induced by root cooling was characterized by a single peak. The increase in Ca^{2+} influx lagged slightly behind the initial depolarizing stimulus. The predicted time course of Ca^{2+} influx was qualitatively similar to the changes in cytoplasmic Ca^{2+} concentration observed when tobacco (Knight et al., 1991, 1993) or *Arabidopsis* seedlings (Knight et al., 1996; Lewis et al., 1997) were cooled. Thus, depolarization-activated, Ca^{2+}-permeable channels, such as the maxi cation channel, could underlie the changes in cytoplasmic Ca^{2+} observed when plants are cooled.

This work was supported by the Biotechnology and Biological Sciences Research Council. We thank our colleagues at HRI for productive discussions on modeling ion channel permeation.

References

Aidley, D.J., Stanfield, P.R. 1996. Ion Channels. Molecules in Action. Cambridge University Press, Cambridge

Allen, G.J., Sanders D., Gradmann, D. 1998. Calcium-potassium selectivity: kinetic analysis of current-voltage relationships of the open, slowly activating channel in the vacuolar membrane of *Vicia faba* guard cells. *Planta* **204:**528–541

Alvarez, O., Villarroel, A., Eisenman, G. 1992. Calculation of ion currents from energy profiles and energy profiles from ion currents in multibarrier, multisite, multioccupancy channel models. *Methods Enzymol.* **207:**816–854

Chilcott, T.C., Shartzer, S.F., Iverson, M.W., Garvin, D.F., Kochian, L.V., Lucas, W.J. 1995. Potassium transport kinetics of *KAT1* expressed in *Xenopus* oocytes: a proposed molecular structure and field effect mechanism for membrane transport. *C. R. Acad. Sci. Paris, Life Sci.* **318:**761–771

Doyle, D.A., Cabral, J.M., Pfuetzner, R.A., Kuo, A., Gulbis, J.M., Cohen, S.L., Chait, B.T., MacKinnon, R. 1998. The structure of the potassium channel: Molecular basis of K^+ conduction and selectivity. *Science* **280:**69–77

Eisenberg, R.S. 1996. Computing the field in proteins and channels. *J. Membrane Biol.* **150:**1–25

French, R.J., Worley, J.F., Wonderlin, W.F., Kularatna, A.S., Kreuger, B.K. 1994. Ion permeation, divalent ion block, and chemical modification of single sodium channels. *J. Gen. Physiol.* **103:**447–470

Gradmann, D., Blatt, M.R., Thiel, G. 1993. Electrocoupling of ion transporters in plants. *J. Membrane Biol.* **136:**327–332

Gradmann, D., Buschmann, P. 1997. Oscillatory interactions between voltage-gated electroenzymes. *J. Exp. Bot.* **48:**399–404

Gradmann, D., Hoffstadt, J. 1998. Electrocoupling of ion transporters in plants: Interaction with internal ion concentrations. *J. Membrane Biol.* **166:**51–59

Gradmann, D., Johannes, E., Hansen, U.-P. 1997. Kinetic analysis of Ca^{2+}/K^+ selectivity of an ion channel by single-binding-site models. *J. Membrane Biol.* **159:**169–178

Gray, P.T.A. 1987. Kinetic analysis of voltage clamp records. *In:* Mi-

croelectrode Techniques. The Plymouth Workshop Handbook. N.B. Standen, P.T.A. Gray and M.J. Whitaker, editors. pp. 41–63. Company of Biologists, Cambridge

Hansen, U.-P., Keunecke, M., Blunck, R. 1997. Gating and permeation models of plant channels. *J. Exp. Bot.* **48:**365–82

Hille, B. 1992. Ionic Channels of Excitable Membranes. Sinauer Associates, Massachusetts

Hille, B., Schwarz, W. 1978. Potassium channels as multi-ion single-file pores. *J. Gen. Physiol.* **72:**409–442

Knight, H., Trewavas, A.J., Knight, M.R. 1996. Cold calcium signalling in *Arabidopsis* involves two cellular pools and a change in calcium signature after acclimation. *Plant Cell* **8:**489–503

Knight, M.R., Campbell, A.K., Smith, S.M., Trewavas, A.J. 1991. Transgenic plant aequorin reports the effects of touch and cold-shock and elicitors on cytoplasmic calcium. *Nature* **352:**524–526

Knight, M.R., Read, N.D., Campbell, A.K., Trewavas, A.J. 1993. Imaging calcium dynamics in living plants using semisynthetic recombinant aequorin. *J. Cell Biol.* **121:**83–90

Latorre, R., Labarca, P., Naranjo, D. 1992. Surface charge effects on ion conduction in ion channels. *Methods Enzymol.* **207:**471–501

Lewis, B.D., Karlin-Neumann, G., Davis, R.W., Spalding, E.P. 1997. Ca^{2+}-activated anion channels and membrane depolarizations induced by blue light and cold in *Arabidopsis* seedlings. *Plant Physiol.* **114:**1327–1334

Margolis, E.J. 1966. Chemical Principles in Calculations of Ionic Equilibria. MacMillan, New York

Marschner, H. 1995. Mineral Nutrition of Higher Plants. Second Edition. Academic Press, London

Minorsky, P.V. 1989. Temperature sensing by plants: a review and hypothesis. *Plant Cell Environ.* **12:**119–135

Minorsky, P.V., Spanswick, R.M. 1989. Electrophysiological evidence for a role for calcium in temperature sensing by roots of cucumber seedlings. *Plant Cell Environ.* **12:**137–143

Nonner, W., Chen, D.P., Eisenberg, B. 1998. Anomalous mole fraction effect, electrostatics, and binding in ionic channels. *Biophys. J.* **74:**2327–2334

Nonner, W., Eisenberg, B. 1998. Ion permeation and glutamate residues linked by Poisson-Nernst-Planck theory in L-type calcium channels. *Biophys. J.* **75:**1287–1305

Robinson, R.A., Stokes, R.H. 1959. Electrolyte Solutions. Butterworths Scientific Publications, London

Tikhonov, D.B., Magazanik, L.G. 1998. Voltage dependence of open channel blockade: onset and offset rates. *J. Membrane Biol.* **161:**1–8

White, P.J. 1993. Characterization of a high-conductance, voltage-dependent cation channel from the plasma membrane of rye roots in planar lipid bilayers. *Planta* **191:**541–551

White, P.J. 1996. Specificity of ion channel inhibitors for the maxi cation channel in rye root plasma membrane. *J. Exp. Bot.* **47:**713–716

White, P.J. 1997. Cation channels in the plasma membrane of rye roots. *J. Exp. Bot.* **48:**499–514

White, P.J. 1998*a*. Calcium channels in the plasma membrane of root cells. *Ann. Bot.* **81:**173–183

White, P.J. 1998*b*. The kinetics of quinine blockade of the maxi cation channel in the plasma membrane of rye roots. *J. Membrane Biol.* **164:**275–281

White, P.J., Ridout, M. 1995. The K^+ channel in the plasma membrane of rye roots has a multiple ion residency pore. *J. Membrane Biol.* **143:**37–49

White, P.J., Ridout, M.S. 1998. The estimation of rapid rate-constants from current-amplitude frequency distributions of single-channel recordings. *J. Membrane Biol.* **161:**115–129